University of Technology and Life Sciences
Bydgoszcz, Poland

Advancements in Electric Machines

Lecture No 7

Axial Flux Permanent Magnet Brushless Machines

Prof. Jacek F. Gieras, *IEEE Fellow*
e-mail: jgieras@ieee.org

Electrical Engineering, Full Time Program, Acad. Year 2009/10

Axial Flux Permanent Magnet Brushless Motors

Outline of the presentation

- Topologies and geometries
- Multidisk axial flux motors
- Coreless axial flux motors
- Halbach array of PMs
- Electromagnetic torque
- Excitation magnetic flux
- EMF
- Sizing equations
- Comparison of cylindrical and disk-type motors
- Commercial axial flux motors
- Applications
- Conclusions
- References

Axial Flux Permanent Magnet Brushless Motors

Topologies and Geometries

(a) Single sided AFPM machines

- with slotted stator
- with slotless stator
- with salient-pole stator

(b) Double sided AFPM machines

- with internal stator
  - with slotted stator
  - with slotless stator
    - with iron core stator
    - with coreless stator
    - without any cores
    - with salient pole stator
  - with internal rotor
    - with slotted stator
    - with slotless stator
    - with salient pole stator

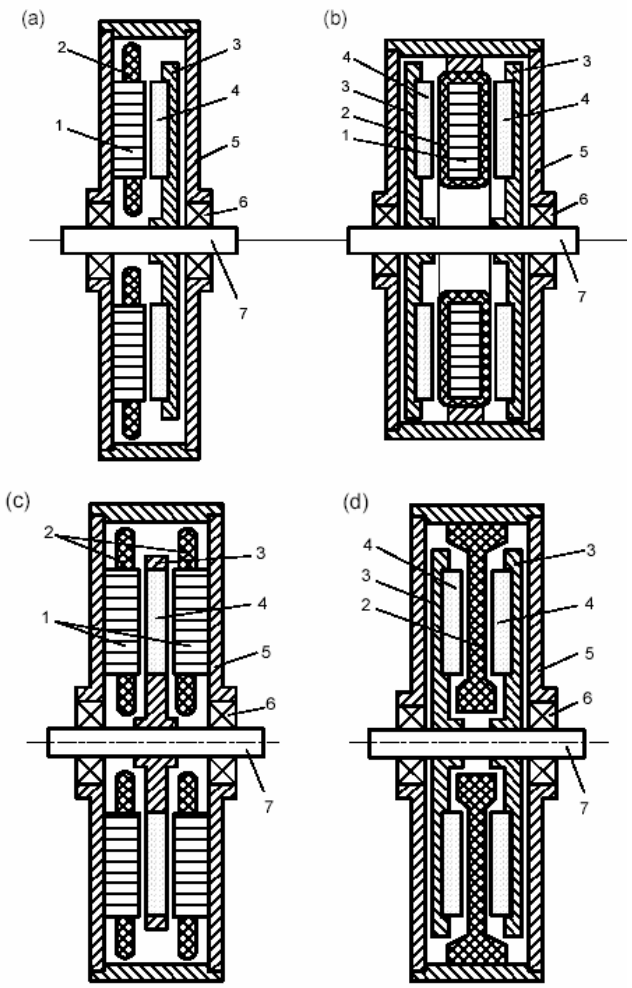

Basic topologies of AFPM machines: (a) single-sided slotted machine, (b) double-sided slotless machine with internal stator and twin PM rotor, (c) double-sided machine with slotted stator and internal PM rotor, (d) double-sided coreless motor with internal stator. 1 – stator core, 2 – stator winding, 3 – rotor, 4 – PM, 5 – frame, 6 – bearing, 7 –shaft.

Axial Flux Permanent Magnet Brushless Motors

Topologies and Geometries

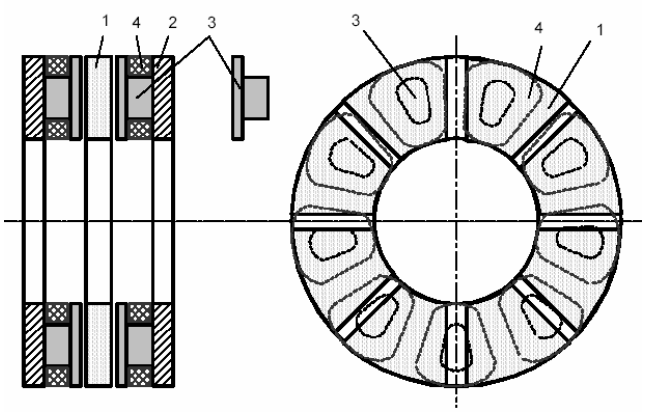

Double-sided AFPM brushless machine with three-phase, 9 –coil external salient-pole stator and 6-pole internal rotor. 1 – PM, 2 – stator backing ferromagnetic disc, 3 – stator pole, 4 – stator coil.

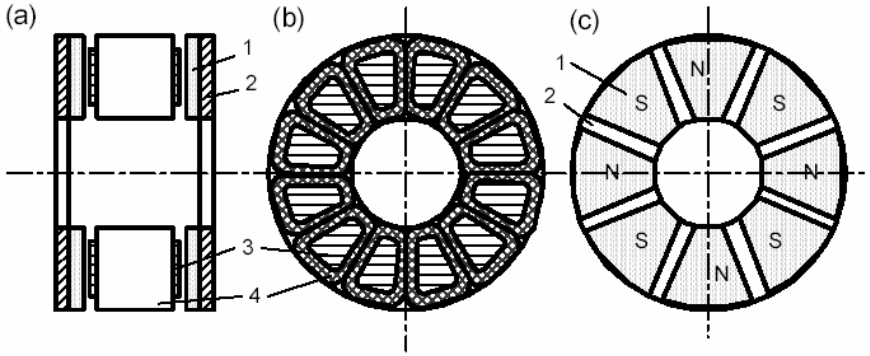

Double-sided AFPM brushless machine with internal salient-pole stator and twin external rotor: (a) construction, (b) stator, (c) rotor. 1- PM, 2 – rotor backing steel disc, 3 – stator pole, 4 – stator coil/

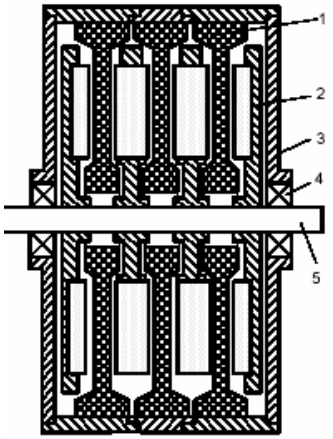

Coreless multidisk AFPM machine with three coreless stators and four PM rotor units: 1 – stator winding, 2 – rotor unit, 3 – frame, 4 – bearing, 5 – shaft.

Axial Flux Permanent Magnet Brushless Motors

Slotted versus slotless

	SLOTTED	SLOTLESS
HIGHER TORQUE DENSITY	?	?
HIGHER EFFICIENCY IN THE LOWER SPEED RANGE	X	
HIGHER EFFICIENCY IN THE HIGHER SPEED RANGE		X
LOWER INPUT CURRENT	X	
LESS PM MATERIAL	X	
LOWER WINDING COST	?	?
LOWER THRUST RIPPLE		X
LOWER ACOUSTIC NOISE		X

Axial Flux Permanent Magnet Brushless Motors

Why multidisk motors?

There is a limit on the increase of the motor torque that can be achieved by enlarging the motor diameter. Factors limiting the single disk design are:

(a) force taken by bearings,

(b) integrity of mechanical joint between the disk and shaft,

(c) disk stiffness.

A reasonable solution for larger torques are double or tripple disk motors.

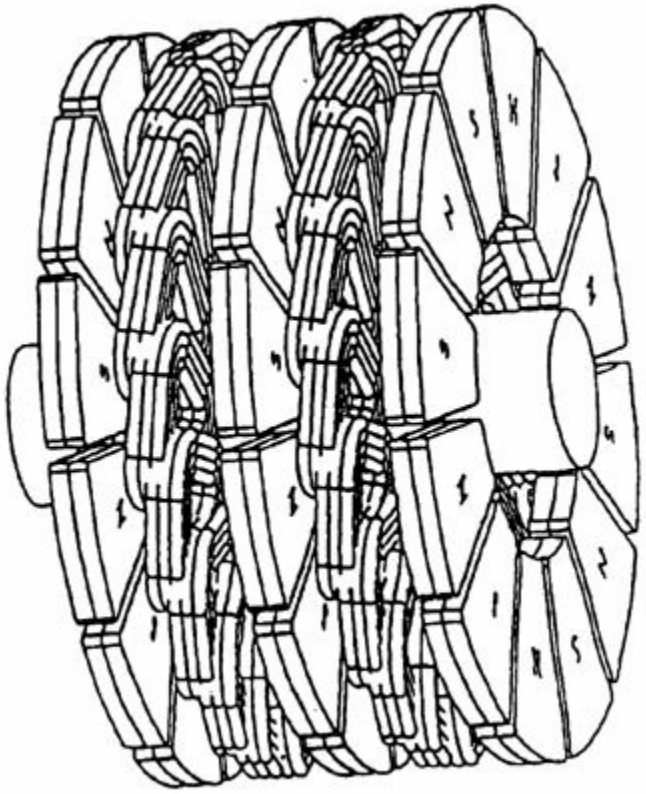

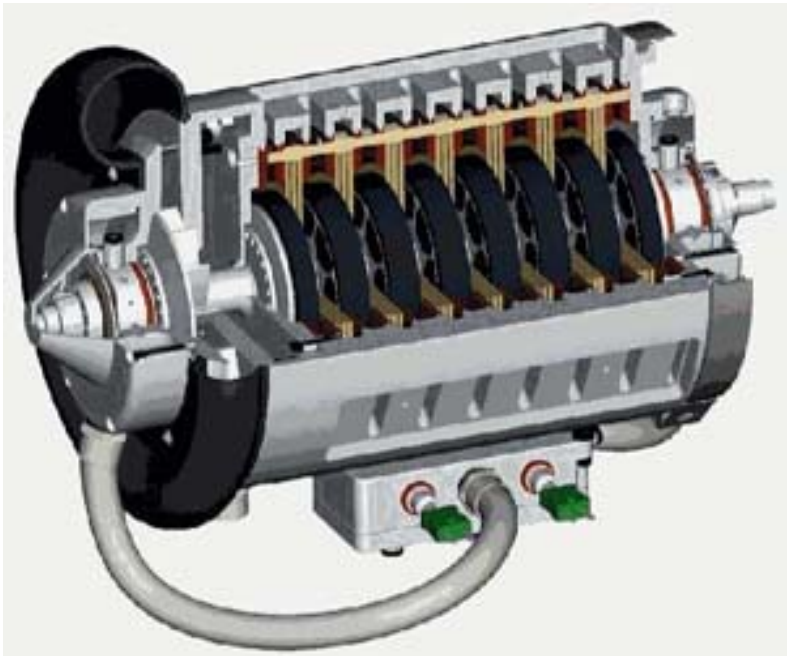

100-kW, 60,000-rpm multi-disk PM brushless generator. Photo courtesy of *Turbo GenSet*, London, U.K.

Axial Flux Permanent Magnet Brushless Motors

Disk Type Coreless PM Brushless Motor

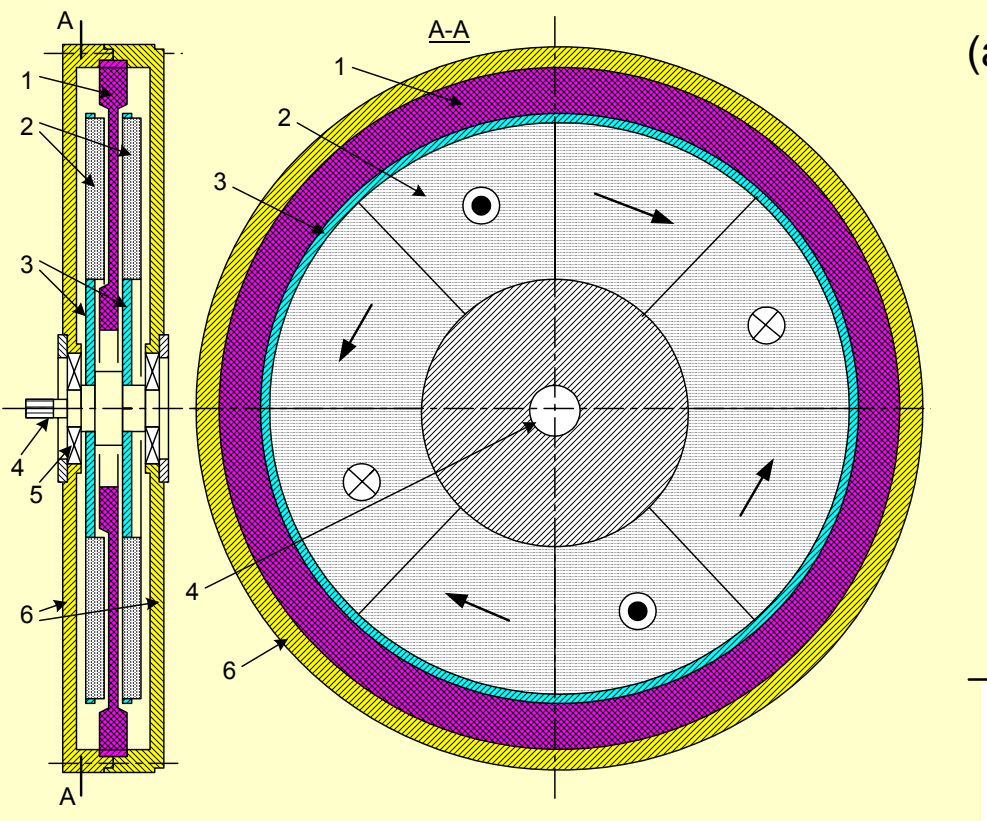

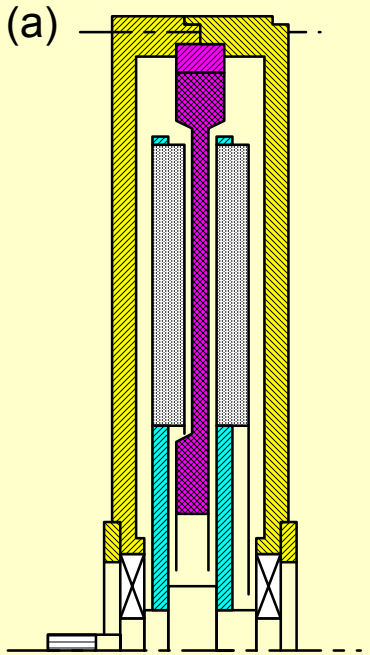

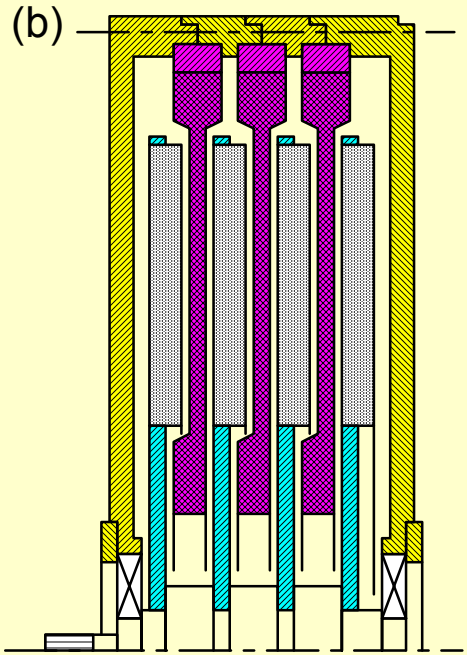

1 - coreless stator (armature) winding,

2 - permanent magnets,

3 - twin rotor, 4 - shaft, 5 bearing, 6 - frame

Segmental construction: (a) single module (segment),

(b) three-module assembly

Axial Flux Permanent Magnet Brushless Mo

Coreless stator coils

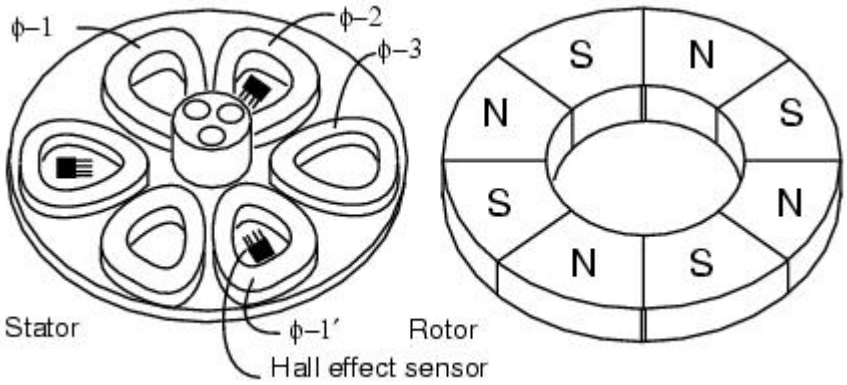

Axial Flux Permanent Magnet Brushless Motors

Disk Type Coreless PM Brushless Motor

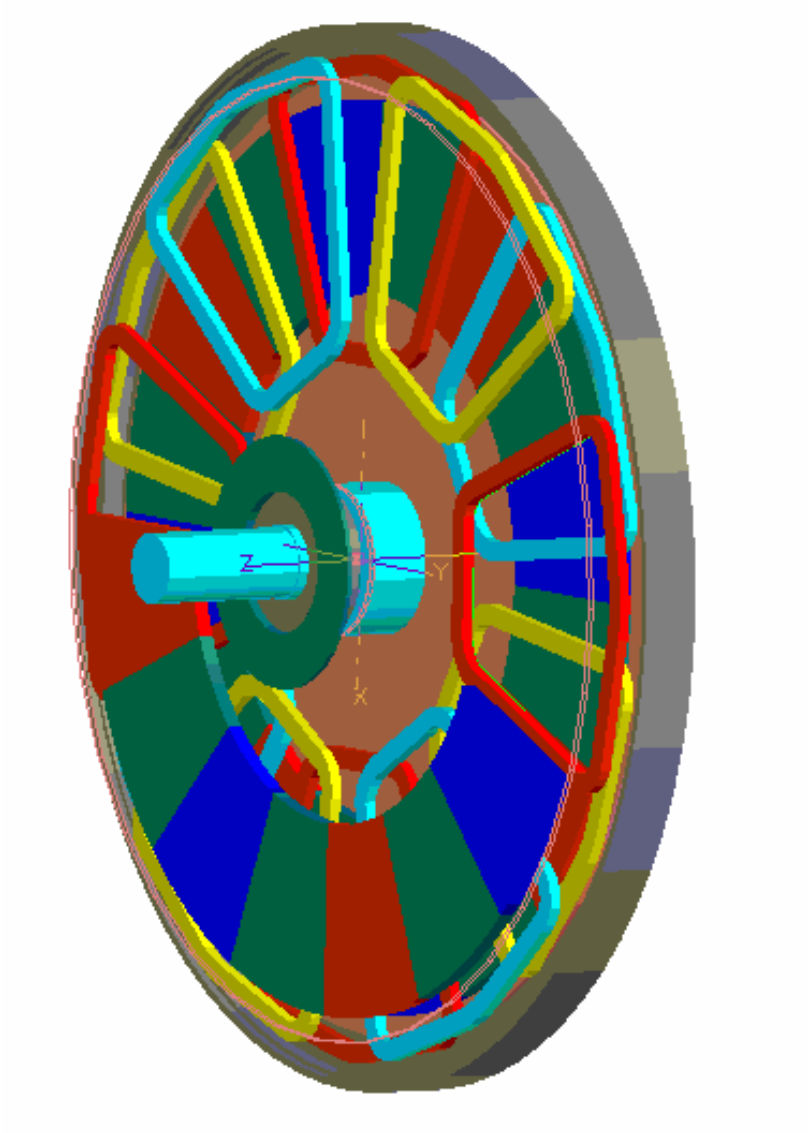

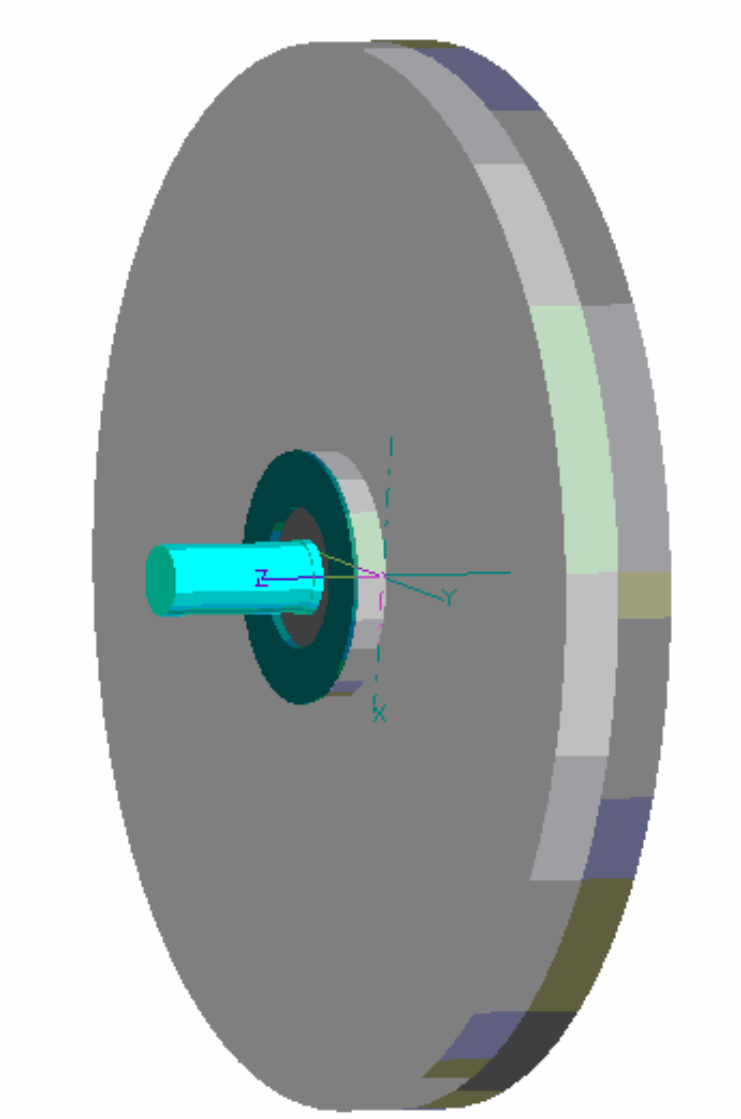

Axial Flux Permanent Magnet Brushless Motors

Disk Type Coreless PM Brushless Motor

(a) Halbach array PM rotor

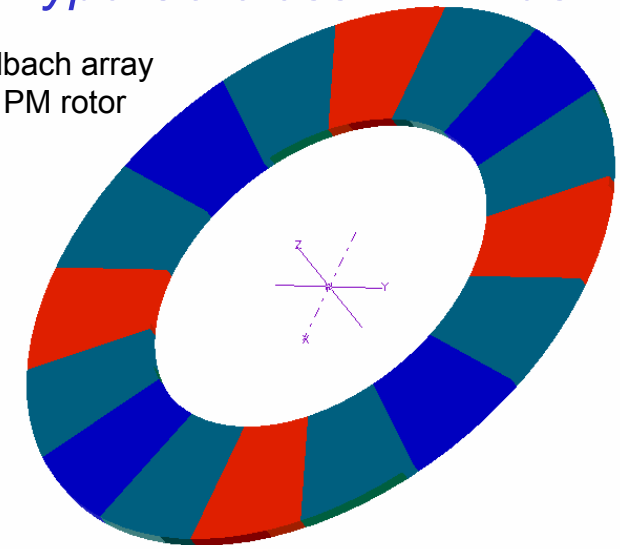

(b) Stator winding

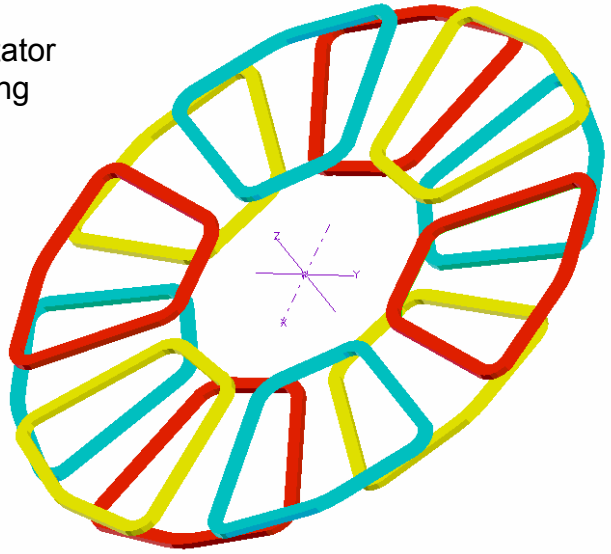

(c) Stator winding and ½ rotor

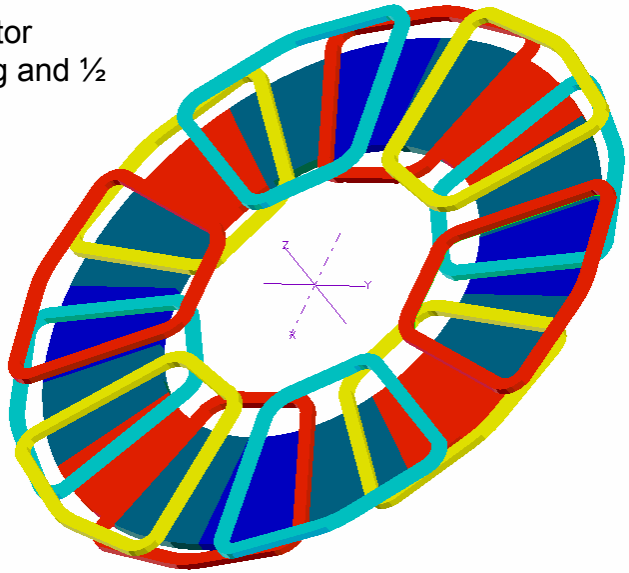

(d) Stator winding and twin rotor

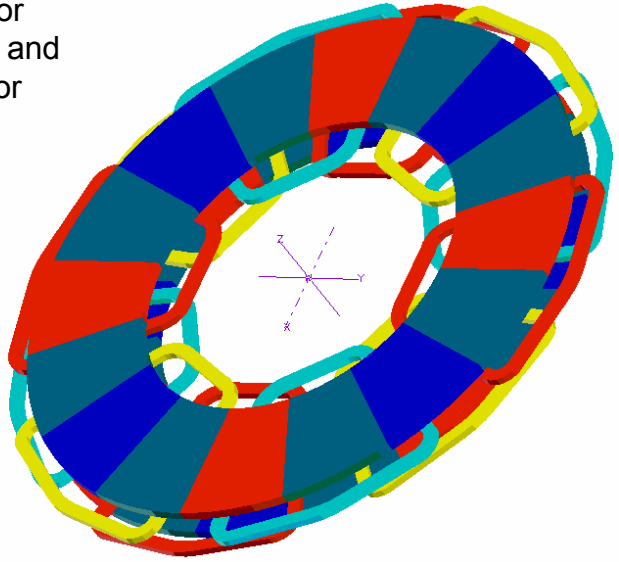

Axial Flux Permanent Magnet Brushless Motors

Polarity of Permanent Magnet Halbach Array

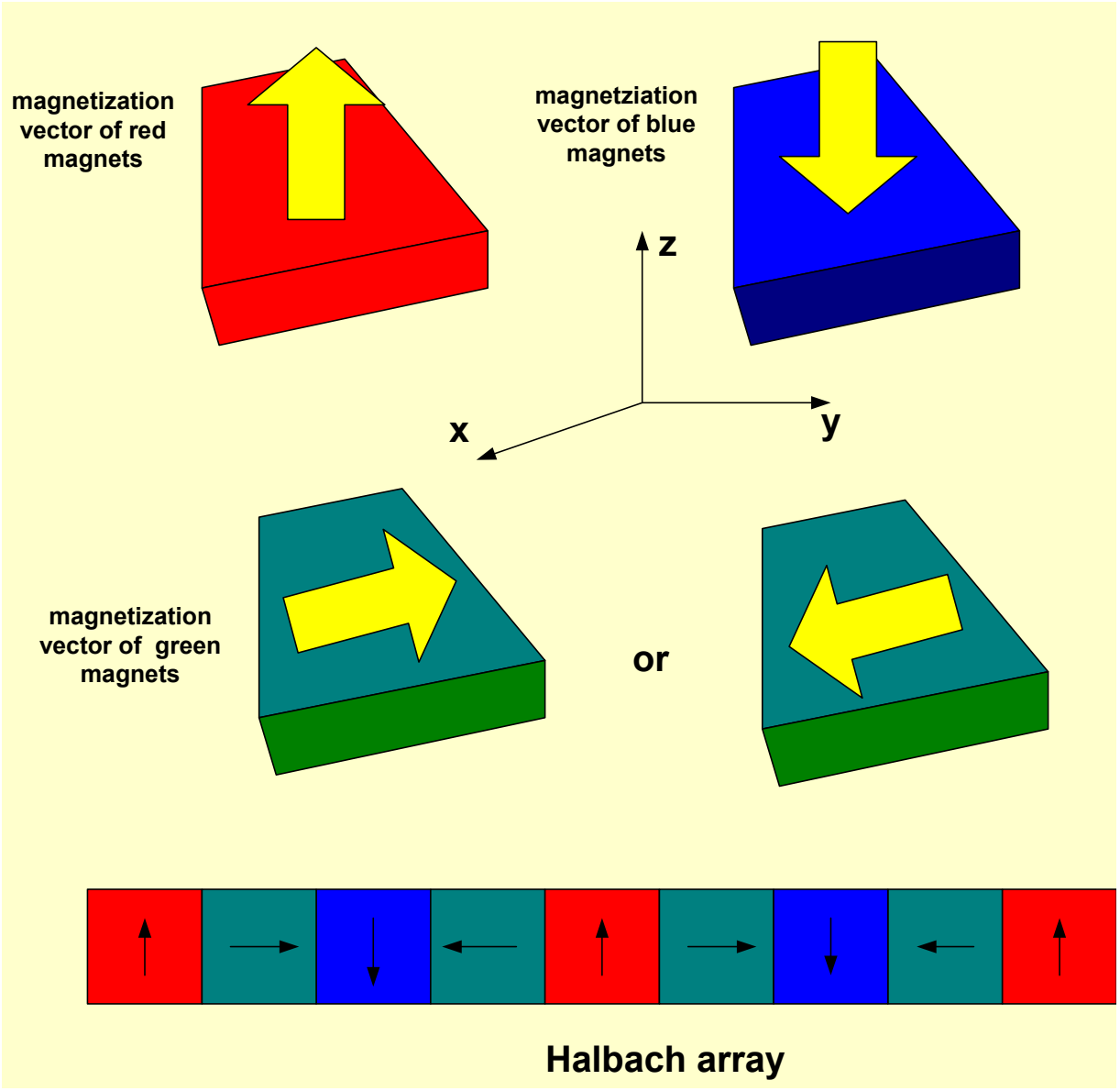

Axial Flux Permanent Magnet Brushless Motors

Polarity of Permanent Magnet Halbach Array

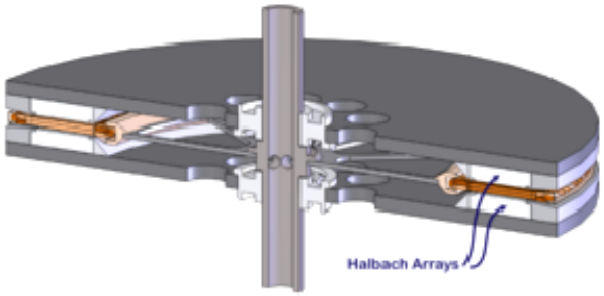

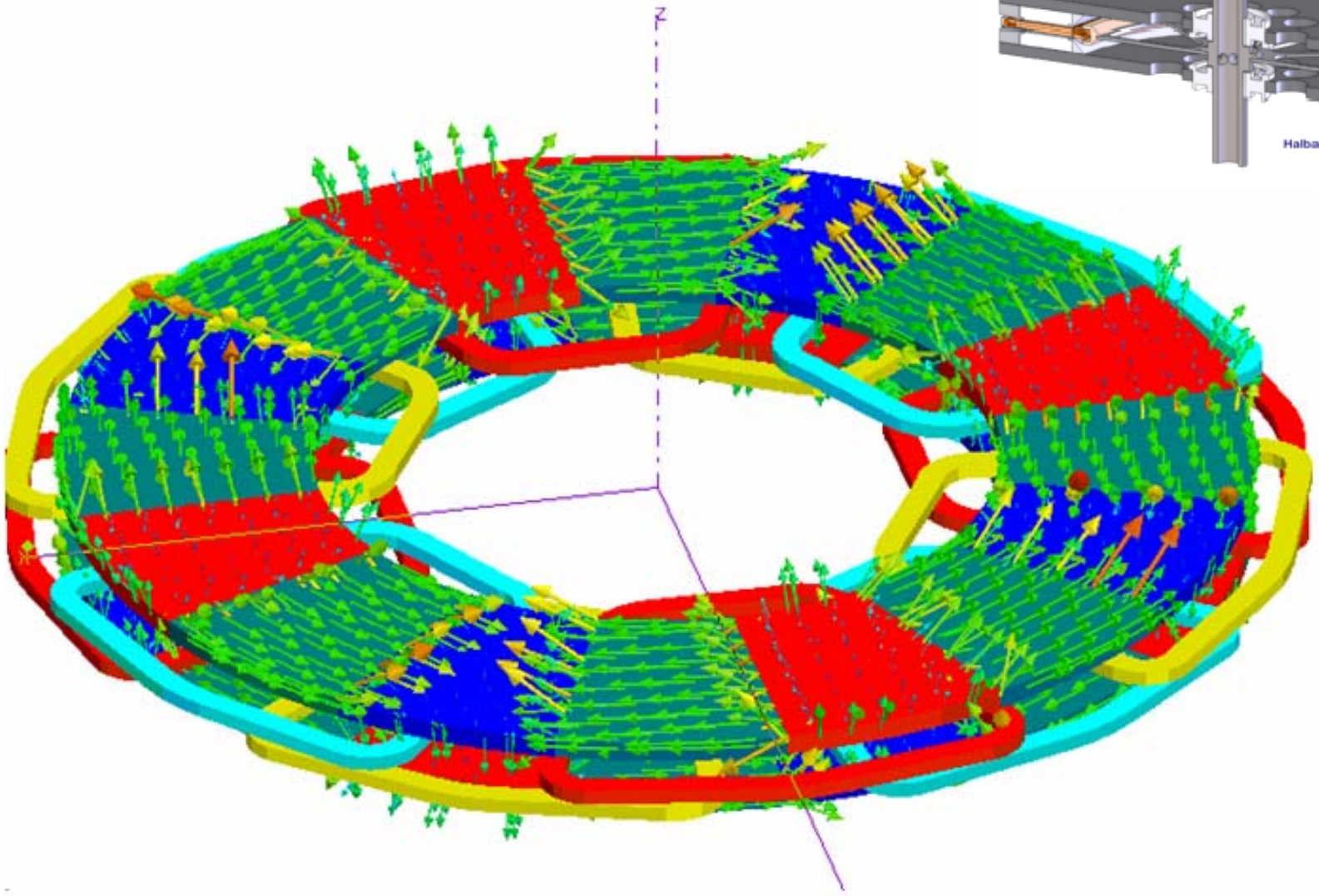

Axial Flux Permanent Magnet Brushless Motors

Halbach Configuration of PMs Provides High Air Gap Magnetic Flux Density without any Ferromagnetic Core

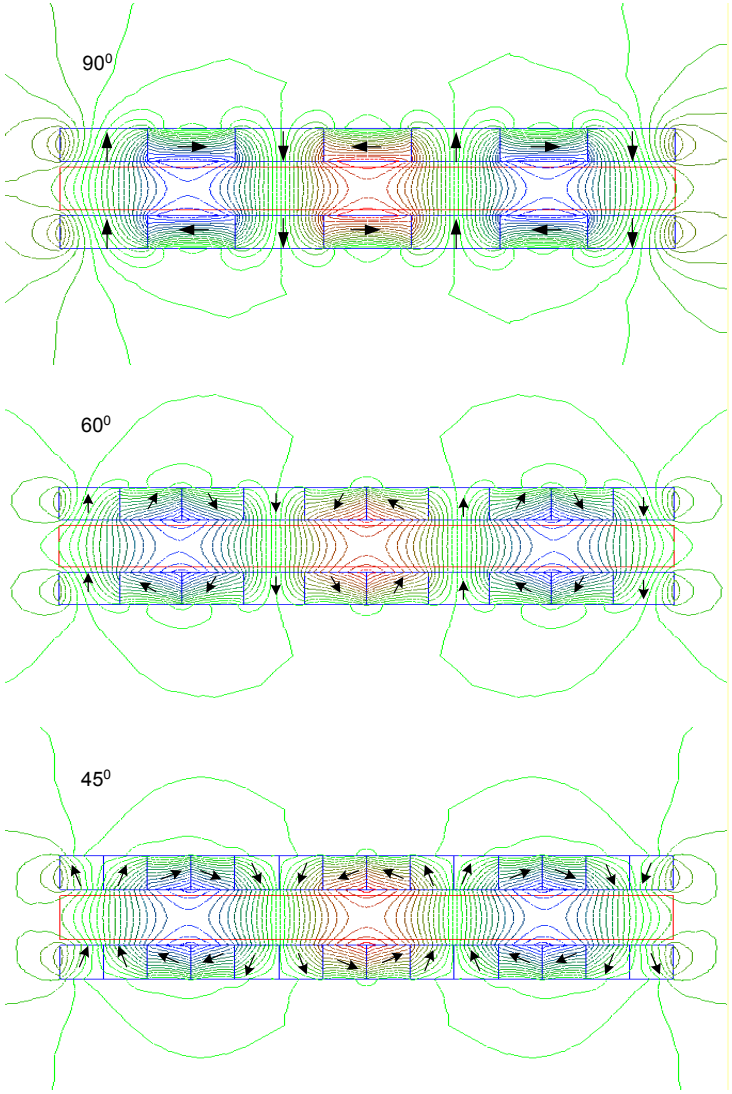

Peak value of normal component of magnetic flux density $B_m \geq$ = 0.6 T at B_r = 1.23 T, H_c = 979 kA/m,

magnet-to-magnet air gap = 10 mm and magnet thickness = 6 mm

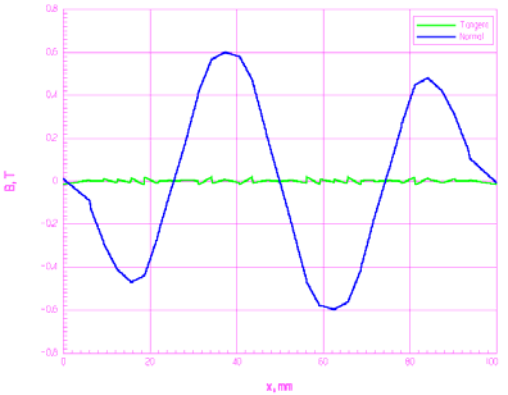

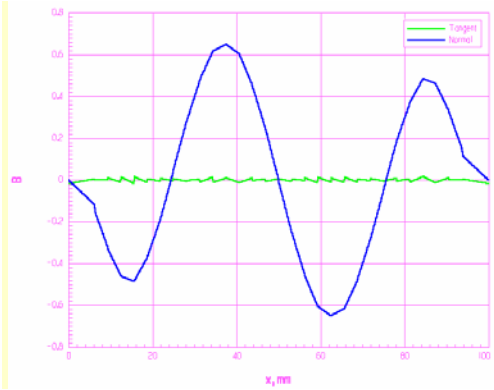

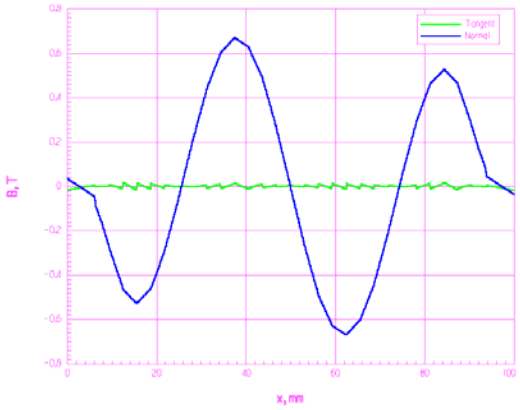

Axial Flux Permanent Magnet Brushless Motors

Disk Type Coreless PM Brushless Motor

ADVANTAGES of coreless machines

- **there is no cogging (detent) torque**
- **the are no forces between the stator and rotor at zero current state**
- **no core losses, no flux pulsation losses due to toothed armature cores, high efficiency**
- **slotless armature (stator) system provides more space for conductors and winding losses can be reduced due to higher conductor cross section**
- **losses due to skin effect in the armature conductors can be reduced by using stranded Litz wires.**
- **the mass of the motor is significantly reduced**

DRAWBACKS of coreless machines

- **the armature (stator) winding inductance is low**
- **large axial forces between two halves of the twin rotor**
- **much higher volume of permanent magnet material in comparison with standard motor**

Excitation Flux

For sinusoidal distribution of the magnetic flux density waveform excited by PMs, the *average magnetic flux density* is

$$B_{avg} = \frac{1}{\pi/p - 0}\int_0^{\pi/p} B_{mg}\sin(p\alpha)d\alpha = -\frac{p}{\pi}B_{mg}\left[\frac{1}{p}\cos(p\alpha)\right]_0^{\pi/p}$$

$$= -\frac{1}{\pi}B_{mg}[\cos\pi - \cos 0] = \frac{2}{\pi}B_{mg} \qquad (2.18)$$

Since the surface element per pole is $2\pi r dr/(2p)$, the magnetic flux excited by PMs per pole for a nonsinusoidal magnetic flux density waveform $B_{avg} = \alpha_i B_{mg}$ is

$$\Phi_f = \int_{R_{in}}^{R_{out}} \alpha_i B_{mg}\frac{2\pi}{2p}r dr = \alpha_i B_{mg}\frac{\pi}{p}\left[\frac{r^2}{2}\right]_{R_{in}}^{R_{out}}$$

$$= \alpha_i B_{mg}\frac{\pi}{2p}(R_{out}^2 - R_{in}^2) \qquad (2.19)$$

where B_{mg} is the *peak value of the magnetic flux density* in the air gap, p is the number of pole pairs, $R_{out} = 0.5D_{out}$ is the outer radius of the PMs and $R_{in} = 0.5D_{in}$ is the inner radius of the PMs.

Excitation Flux

It is convenient to use the *inner–to–outer PM radius* or *inner–to–outer PM diameter* ratio, i.e.

$$k_d = \frac{R_{in}}{R_{out}} = \frac{D_{in}}{D_{out}} \tag{2.20}$$

Thus,

$$\Phi_f = \alpha_i B_{mg} \frac{\pi}{2p} [(0.5D_{out})^2 - (0.5D_{in})^2] = \alpha_i B_{mg} \frac{\pi}{8p} D_{out}^2 (1 - k_d^2) \tag{2.21}$$

The same equation for a cylindrical type machine is [96]

$$\Phi_f = \frac{2}{\pi} \tau L_i B_{mg} \tag{2.22}$$

where τ is the pole pitch and L_i is the effective length of the stack.

Electromagnetic Torque

The *line current density* is also a function of the radius r. Thus the peak value of the line current density is

$$A_m(r) = \frac{m_1\sqrt{2}N_1I_a}{p\tau(r)} = \frac{m_1\sqrt{2}N_1I_a}{\pi r} \tag{2.15}$$

The *tangential force* acting on the disc can be calculated on the basis of Ampere's equation

$$d\vec{F}_x = I_a(d\vec{r} \times \vec{B}_g) = A(r)(d\vec{S} \times \vec{B}_g) \tag{2.16}$$

where $I_a d\vec{r} = A(r)d\vec{S}$, $A(r) = A_m(r)/\sqrt{2}$ according to eqn (2.15), $d\vec{r}$ is the radius element, $d\vec{S}$ is the surface element and $\vec{B}_g$ is the vector of the normal component (perpendicular to the disc surface) of the magnetic flux density in the air gap. An AFPM disc-type machine provides $\vec{B}_g$ practically independent of the radius r.

Assuming the magnetic flux density in the air gap B_{mg} is independent of the radius r, $dS = 2\pi r dr$ and $B_{avg} = \alpha_i B_{mg}$ according to eqn (2.14), the electromagnetic torque on the basis of eqn (2.16) is

$$dT_d = rdF_x = r[k_{w1}A(r)B_{avg}dS] = 2\pi\alpha_i k_{w1}A(r)B_{mg}r^2dr \tag{2.17}$$

Electromagnetic Torque

The *average electromagnetic torque* developed by AFPM motor according to eqns (2.15) and (2.17) is

$$dT_d = 2\alpha_i m_1 I_a N_1 k_{w1} B_{mg} r dr$$

If the above equation is integrated from $D_{out}/2$ to $D_{in}/2$ with respect to r, the average electromagnetic torque may be written as

$$\begin{aligned} T_d &= \frac{1}{4}\alpha_i m_1 I_a N_1 k_{w1} B_{mg}(D_{out}^2 - D_{in}^2) \\ &= \frac{1}{4}\alpha_i m_1 N_1 k_{w1} B_{mg} D_{out}^2 (1 - k_d^2) I_a \end{aligned} \qquad (2.24)$$

where k_d is according to eqn (2.20). Putting eqn (2.21) into eqn (2.24) the average torque is

$$T_d = 2\frac{p}{\pi} m_1 N_1 k_{w1} \Phi_f I_a \qquad (2.25)$$

Electromagnetic Torque

To obtain the rms torque for sinusoidal current and sinusoidal magnetic flux density, eqn (2.25) should be multiplied by the coefficient $\pi\sqrt{2}/4 \approx 1.11$, i.e.

$$T_d = \frac{m_1}{\sqrt{2}} p N_1 k_{w1} \Phi_f I_a = k_T I_a \tag{2.26}$$

where the *torque constant*

$$k_T = \frac{m_1}{\sqrt{2}} p N_1 k_{w1} \Phi_f \tag{2.27}$$

In some publications [84, 218] the electromagnetic force on the rotor is simply calculated as the product of the magnetic and electric loading $B_{avg}A$ and active surface of PMs $S = \pi(R_{out}^2 - R_{in}^2)$, i.e. $F_x = \pi B_{avg} A (R_{out}^2 - R_{in}^2)$, where A is the rms line current density at the inner radius R_{in}. For a double-sided AFPM machine $S = 2\pi(R_{out}^2 - R_{in}^2)$. Thus, the average electromagnetic torque of a double-sided AFPM machine is

$$T_d = F_x R_{in} = 2\pi B_{avg} A (R_{out}^2 - R_{in}^2) R_{in} = 2\pi B_{avg} A R_{out}^3 (k_d - k_d^3) \tag{2.28}$$

Taking the first derivative of the electromagnetic torque T_d with respect to k_d and equating it to zero, the maximum torque is for $k_d = 1/\sqrt{3}$. Industrial practice shows that the maximum torque is for $k_d \neq 1/\sqrt{3}$.

Axial Flux Permanent Magnet Brushless Motors

EMF

The *EMF at no load* can be found by differentiating the first harmonic of the magnetic flux waveform $\Phi_{f1} = \Phi_f \sin \omega t$ and multiplying by $N_1 k_{w1}$, i.e.

$$e_f = N_1 k_{w1} \frac{d\Phi_{f1}}{dt} = 2\pi f N_1 k_{w1} \Phi_f \cos \omega t$$

The magnetic flux Φ_f is expressed by eqns (2.19) and (2.21). The rms value is obtained by dividing the peak value $2\pi f N_1 k_{w1} \Phi_f$ of the EMF by $\sqrt{2}$, i.e.

$$E_f = \pi\sqrt{2} f N_1 k_{w1} \Phi_f = \pi\sqrt{2} p N_1 k_{w1} \Phi_f n_s = k_E n_s \qquad (2.29)$$

where the *EMF constant* (armature constant) is

$$k_E = \pi\sqrt{2} p N_1 k_{w1} \Phi_f \qquad (2.30)$$

The same form of eqn (2.29) can be obtained on the basis of the developed torque $T_d = m_1 E_f I_a/(2\pi n_s)$ in which T_d is according to eqn (2.26). For the drum type winding the winding factor $k_{w1} = 1$.

Axial Flux Permanent Magnet Brushless Motors

Sizing Equations

The peak line current density at the average radius per one stator is expressed by eqn (2.15) in which the radius may be replaced by an average diameter

$$D = 0.5(D_{out} + D_{in}) = 0.5D_{out}(1 + k_d) \tag{2.85}$$

where D_{out} is the outer diameter, D_{in} is the inner diameter of the stator core and $k_d = D_{in}/D_{out}$ (according to eqn (2.20)). Thus,

$$A_m = \frac{4\sqrt{2}m_1 I_a N_1}{\pi D_{out}(1 + k_d)} \tag{2.86}$$

The EMF induced in the stator winding by the rotor excitation system, according to eqns (2.29) and (2.21) has the following form

$$E_f = \pi\sqrt{2}n_s p N_1 k_{w1}\Phi_f = \frac{\pi}{4}\sqrt{2}n_s N_1 k_{w1} B_{mg} D_{out}^2(1 - k_d^2) \tag{2.87}$$

Sizing Equations

The apparent electromagnetic power in two stators is

$$\begin{aligned} S_{elm} &= m_1(2E_f)I_a = m_1E_f(2I_a) \\ &= \frac{\pi^2}{8}k_{w1}n_sB_{mg}A_mD_{out}^3(1+k_d)(1-k_d^2) \end{aligned} \tag{2.88}$$

For series connection the EMF is equal to $2E_f$ and for parallel connection the current is equal to $2I_a$. For a multidisc motor the number "2" should be replaced by the number of stators. Putting

$$k_D = \frac{1}{8}(1+k_d)(1-k_d^2) \tag{2.89}$$

the apparent electromagnetic power is

$$S_{elm} = \pi^2 k_D k_{w1} n_s B_{mg} A_m D_{out}^3 \tag{2.90}$$

Sizing Equations

The apparent electromagnetic power expressed in terms of active output power is thus

$$S_{elm} = \epsilon \frac{P_{out}}{\eta \cos \phi} \tag{2.91}$$

where the *phase EMF–to–phase voltage* ratio is

$$\epsilon = \frac{E_f}{V_1} \tag{2.92}$$

For motors $\epsilon < 1$ and for generators $\epsilon > 1$.

In connection with eqns (2.90) and (2.91), the PM outer diameter (equal to the outer diameter of the stator core) is

$$D_{out} = \sqrt[3]{\frac{\epsilon P_{out}}{\pi^2 k_D k_{w1} n_s B_{mg} A_m \eta \cos \phi}} \tag{2.93}$$

Sizing Equations

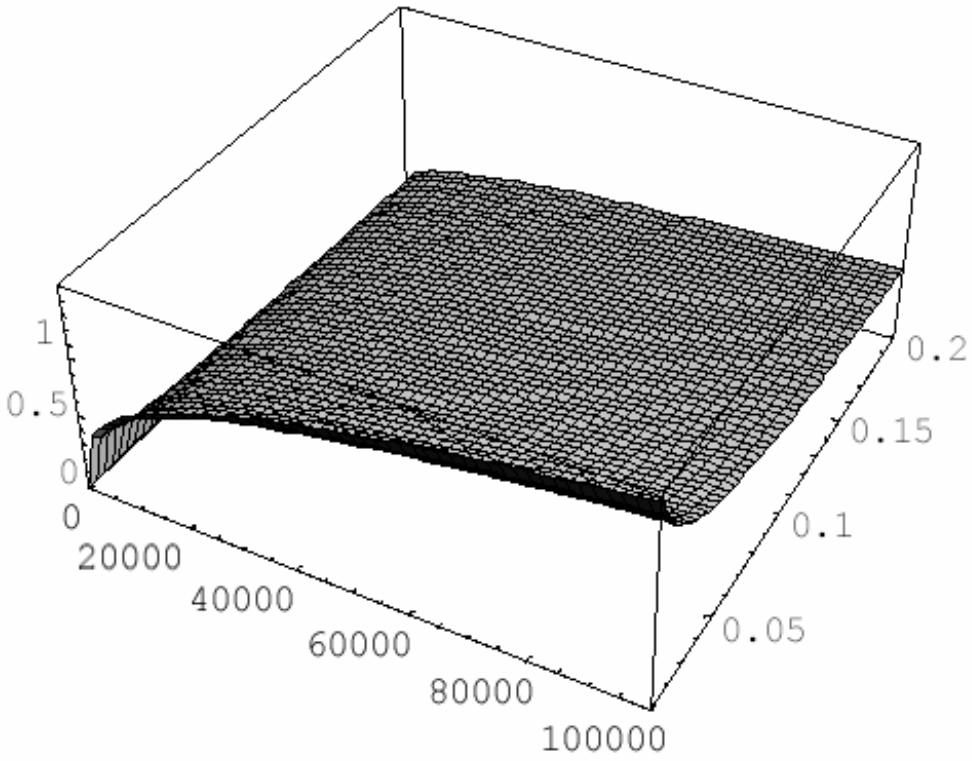

Outer diameter D_{out} as a function of the output power P_{out} and parameter k_D for $\varepsilon = 0.9$, $k_{w1}\eta \cos\phi = 0.84$, n_s = 1000 rpm = 16.67 rev/s and $B_{mg}A_m$ = 26,000 TA/m.

Axial Flux Permanent Magnet Brushless Motors

Sizing Equations

The outer diameter of PMs is the most important dimension of disc rotor PM motors. Since $D_{out} \propto \sqrt[3]{P_{out}}$ the outer diameter increases rather slowly with the increase of the output power (Fig. 2.16). This is why small power disc motors have relatively large diameters. The disc-type construction is preferred for medium and large power motors. Motors with output power over 10 kW have reasonable diameters. Also, disc construction is recommended for a.c. servo motors fed with high frequency voltage.

The electromagnetic torque is proportional to D_{out}^3, i.e.

$$T_d = \frac{P_{elm}}{2\pi n_s} = \frac{S_{elm}\cos\Psi}{2\pi n_s} = \frac{\pi}{2} k_D k_{w1} D_{out}^3 B_{mg} A_m \cos\Psi \qquad (2.94)$$

where P_{elm} is the active electromagnetic power and Ψ is the angle between the stator current I_a and EMF E_f.

Axial Flux Permanent Magnet Brushless Motors

Phasor diagram for overexcited motor

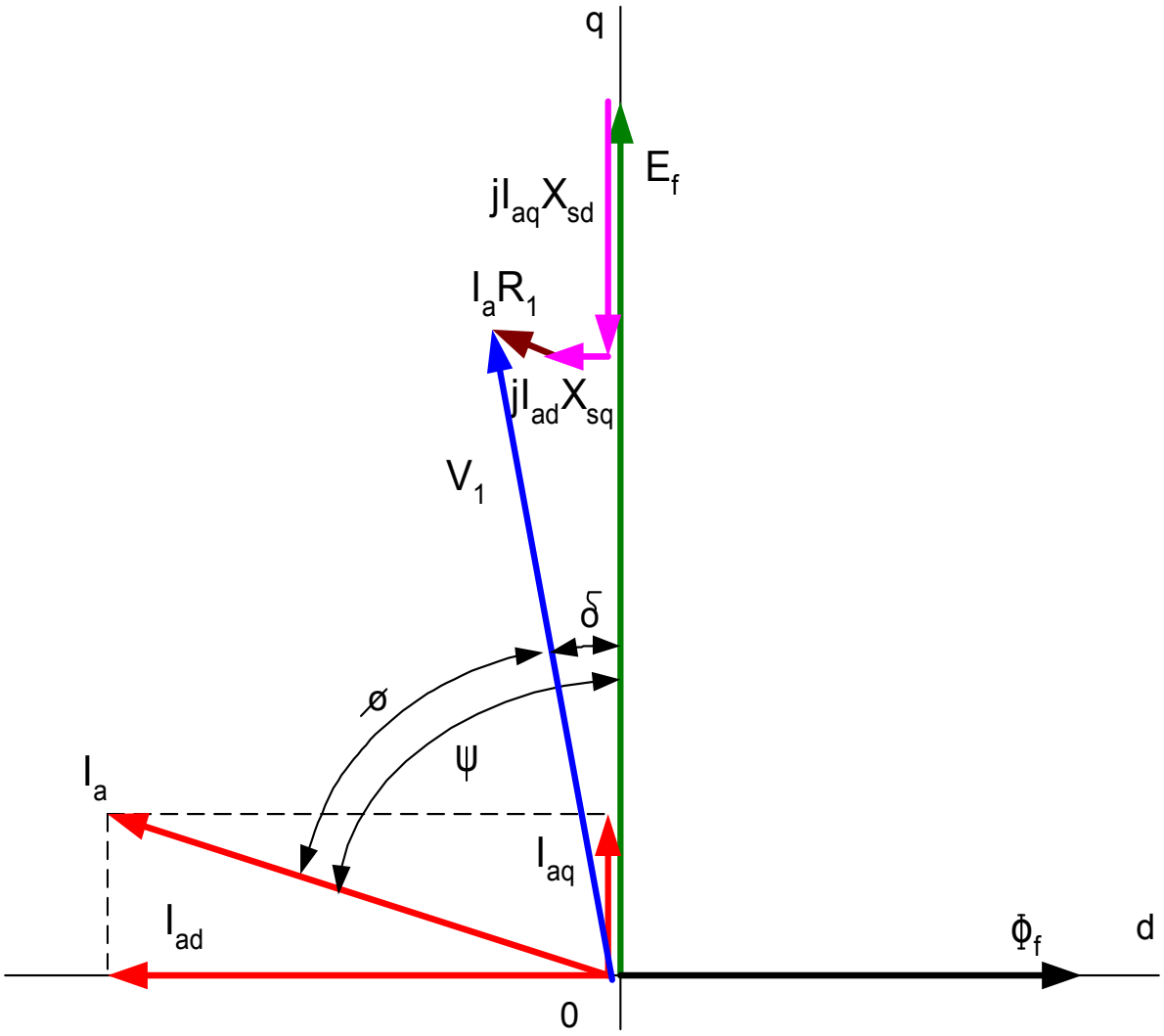

Axial Flux Permanent Magnet Brushless Motors

Armature Reaction Equations for Cylindrical and Disc-Type Motors

Quantity	Cylindrical machine	Disc-type machine
Armature reaction magnetic flux in the d-axis	$\Phi_{ad} = \frac{2}{\pi} B_{mad1} \tau L_i$	$\Phi_{ad} = \frac{2}{\pi} B_{mad1} \frac{\pi}{2p} (R_{out}^2 - R_{in}^2)$
Armature reaction magnetic flux in the q-axis	$\Phi_{aq} = \frac{2}{\pi} B_{maq1} \tau L_i$	$\Phi_{aq} = \frac{2}{\pi} B_{maq1} \frac{\pi}{2p} (R_{out}^2 - R_{in}^2)$
Permeance of the air gap in the d-axis	$\Lambda_d = \frac{\mu_0}{g'} \frac{2}{\pi} \tau L_i$	$\Lambda_d = \frac{\mu_0}{g'} \frac{2}{\pi} \frac{\pi}{2p} (R_{out}^2 - R_{in}^2)$
Permeance of the air gap in the q-axis	$\Lambda_q = \frac{\mu_0}{g'_q} \frac{2}{\pi} \tau L_i$	$\Lambda_q = \frac{\mu_0}{g'_q} \frac{2}{\pi} \frac{\pi}{2p} (R_{out}^2 - R_{in}^2)$
Permeance of the air gap per surface of one pole in the d-axis	$\lambda_d = \frac{\mu_0}{g'}$	
Permeance of the air gap per surface area of one pole in the q-axis	$\lambda_q = \frac{\mu_0}{g'_q}$	

Axial Flux Permanent Magnet Brushless Motors

Armature Reaction Equations for Cylindrical and Disc-Type Motors

Quantity	Cylindrical machine	Disc-type machine
Armature reaction reactance in the d-axis	$X_{ad} = \frac{E_{ad}}{I_{ad}}$ $= 4m_1\mu_0 f \frac{(N_1 k_{w1})^2}{\pi p} \frac{\tau L_i}{g'} k_{fd}$	$X_{ad} = \frac{E_{ad}}{I_{ad}}$ $= 2m_1\mu_0 f \left(\frac{N_1 k_{w1}}{p}\right)^2 \frac{R_{out}^2 - R_{in}^2}{g'} k_{fd}$
Armature reaction reactance in the q-axis	$X_{aq} = \frac{E_{aq}}{I_{aq}}$ $= 4m_1\mu_0 f \frac{(N_1 k_{w1})^2}{\pi p} \frac{\tau L_i}{g'_q} k_{fq}$	$X_{aq} = \frac{E_{aq}}{I_{aq}}$ $= 2m_1\mu_0 f \left(\frac{N_1 k_{w1}}{p}\right)^2 \frac{R_{out}^2 - R_{in}^2}{g'_q} k_{fq}$
Armature reaction inductance in the d-axis	$L_{ad} = \frac{\Psi_{ad}}{I_{ad}}$ $= 2m_1\mu_0 \frac{(N_1 k_{w1})^2}{\pi^2 p} \frac{\tau L_i}{g'} k_{fd}$	$L_{ad} = \frac{\Psi_{ad}}{I_{ad}}$ $= m_1\mu_0 \frac{1}{\pi} \left(\frac{N_1 k_{w1}}{p}\right)^2 \frac{R_{out}^2 - R_{in}^2}{g'} k_{fd}$
Armature reaction inductance in the q-axis	$L_{aq} = \frac{\Psi_{aq}}{I_{aq}}$ $= 2m_1\mu_0 \frac{(N_1 k_{w1})^2}{\pi^2 p} \frac{\tau L_i}{g'_q} k_{fq}$	$L_{aq} = \frac{\Psi_{aq}}{I_{aq}}$ $= m_1\mu_0 \frac{1}{\pi} \left(\frac{N_1 k_{w1}}{p}\right)^2 \frac{R_{out}^2 - R_{in}^2}{g'_q} k_{fq}$

Axial Flux Permanent Magnet Brushless Motors

Commercial Axial Flux PM Motor with inner rotor

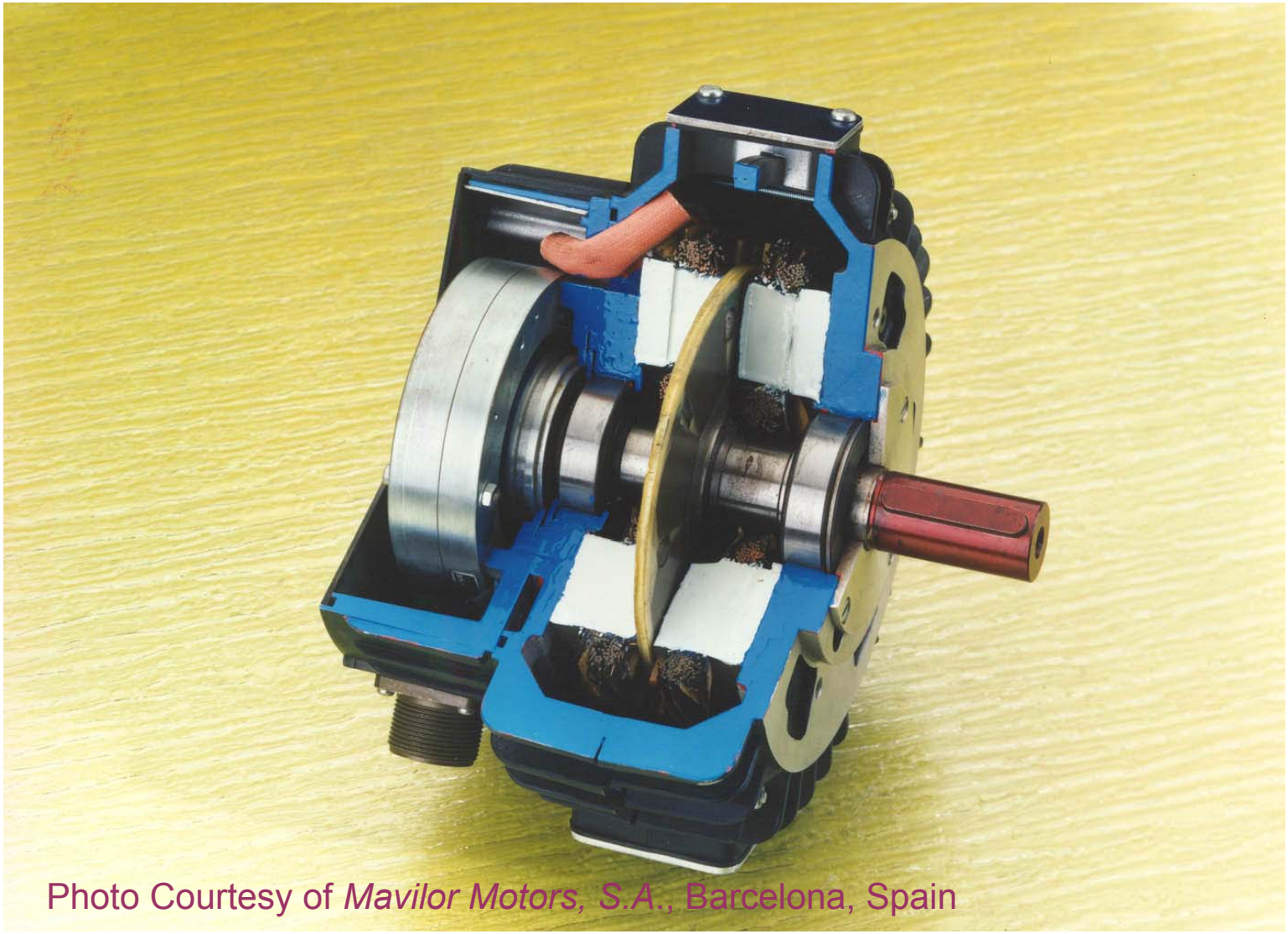

Photo Courtesy of *Mavilor Motors, S.A.*, Barcelona, Spain

Axial Flux Permanent Magnet Brushless Motors

Commercial Axial Flux PM Motor with inner rotor

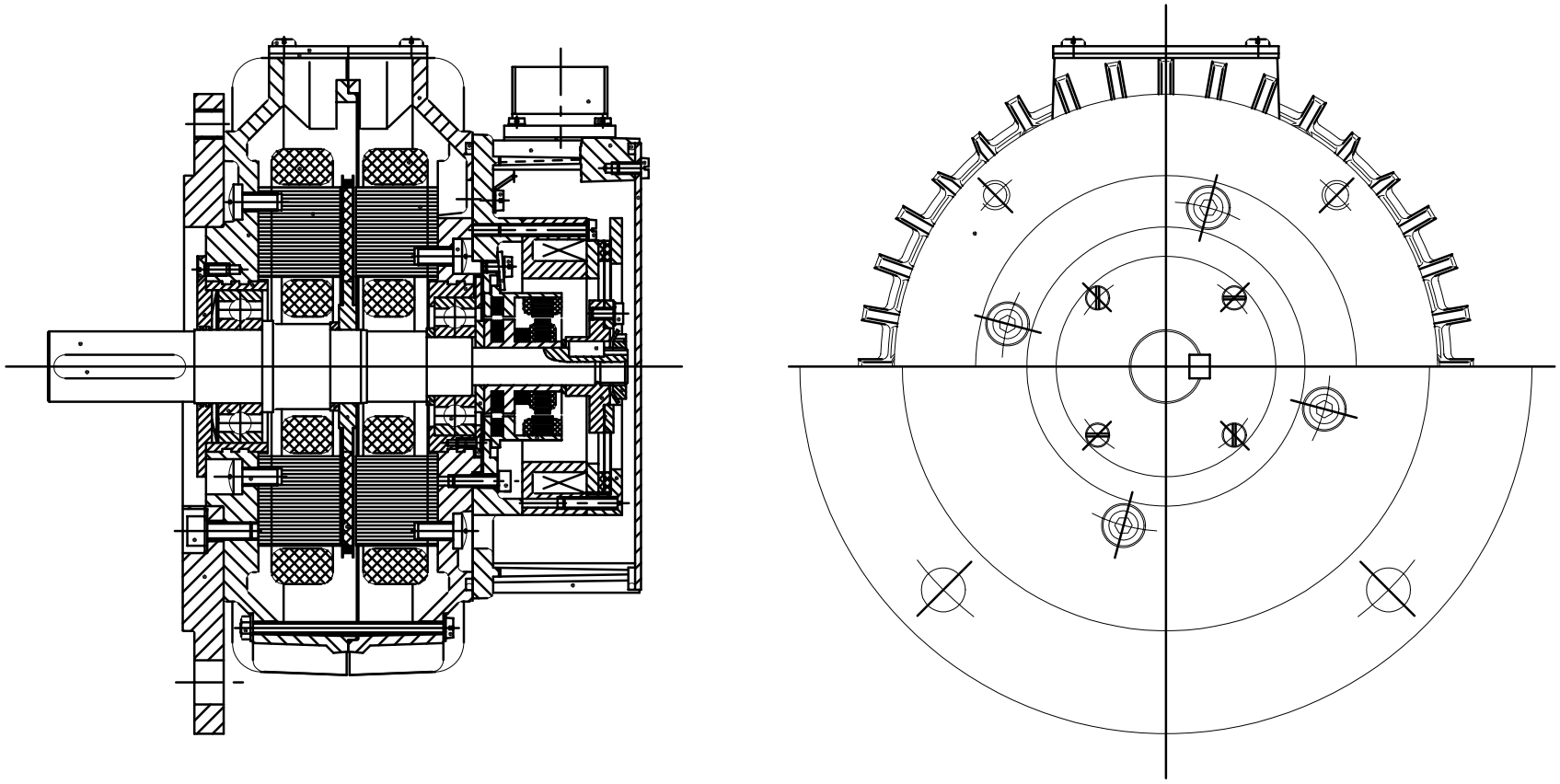

Longitudinal section of the double-sided AFPM brushless servo motor. Courtesy of *Mavilor Motors, S.A.*, Barcelona, Spain.

Axial Flux Permanent Magnet Brushless Motors

Commercial e-Torque™ Motor with Coreless Stator.

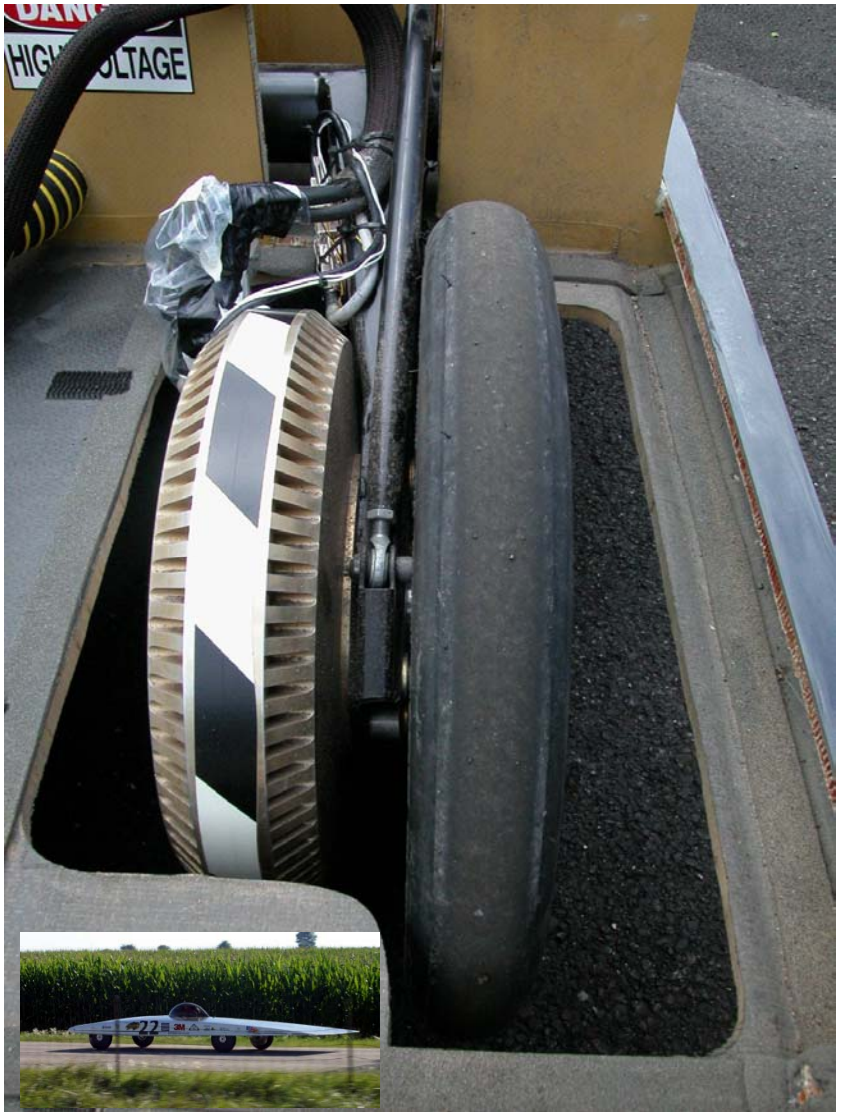

Photo courtesy of *Bodine-Electric Company,* Chicago, IL, U.S.A.

Axial Flux Permanent Magnet Brushless Motors

Commercial e-Torque™ Motor with Coreless Stator – Exploded View

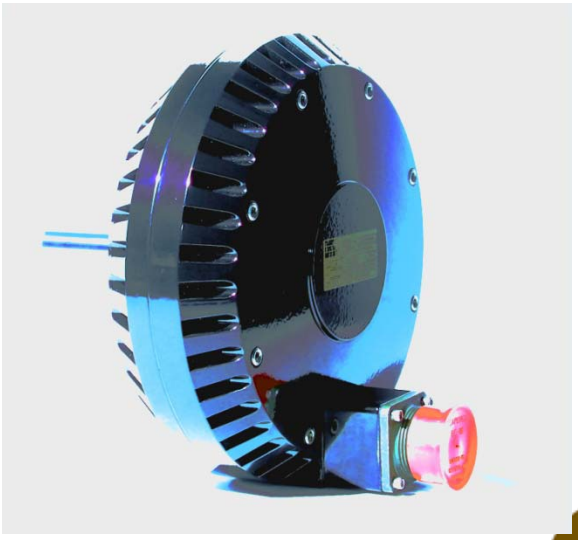

Photo courtesy of *Bodine-Electric Company,* Chicago, IL, U.S.A

Axial Flux Permanent Magnet Brushless Motors

Commercial Miniature Coreless Motor with Film Coil Stator Winding

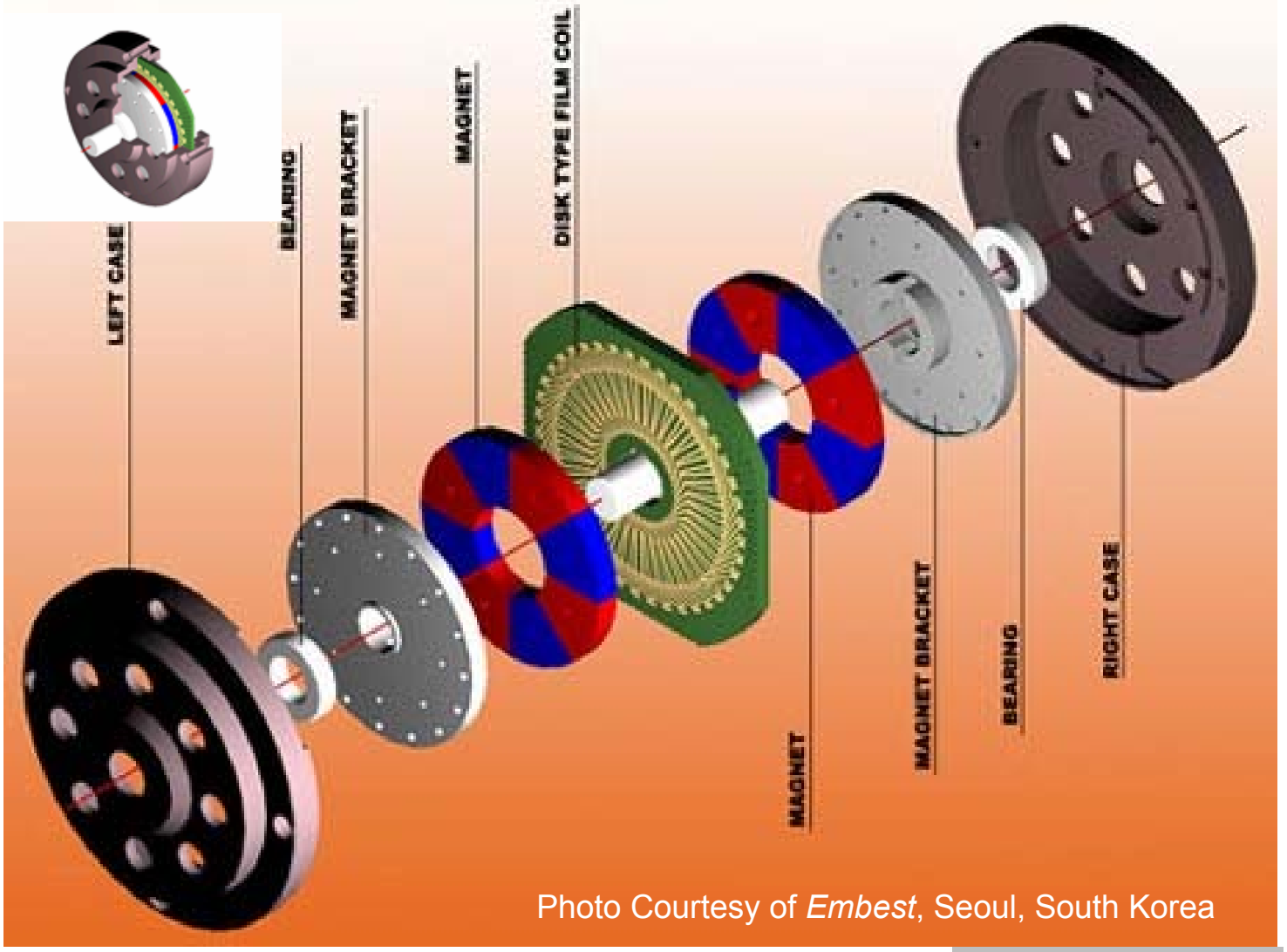

Photo Courtesy of *Embest*, Seoul, South Korea

EMBEST

Axial Flux Permanent Magnet Brushless Motors

Applications: Axial Flux PMBMs in Hybrid Electric Vehicles

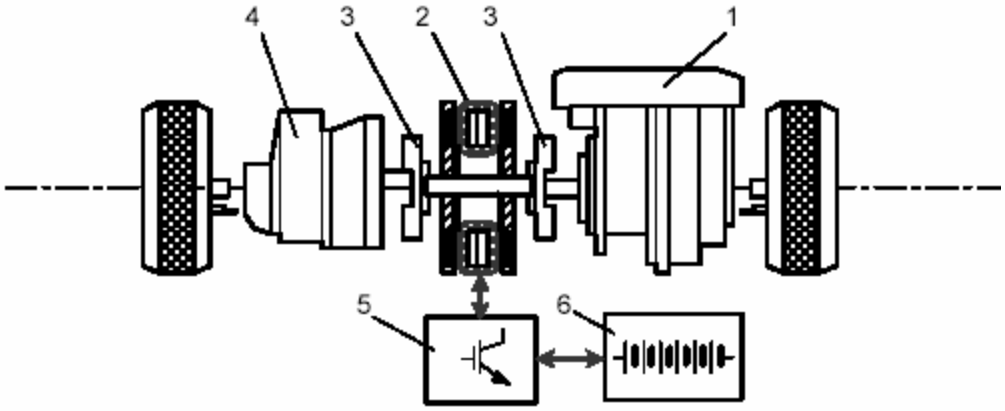

Hybrid-electric gasoline car: 1 – gasoline combustion engine, 2 – integrated motor-generator, 3 – cranking clutch, 4 – gearbox, 5 – inverter, 6 – battery.

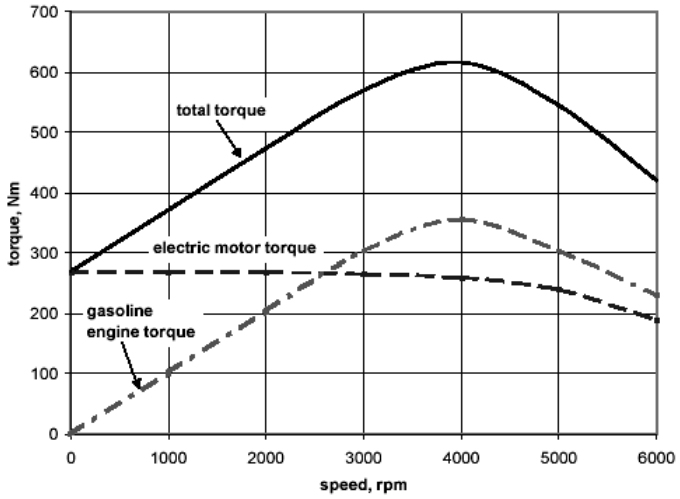

Torque-speed characteristic of an electric motor and gasoline engine. The electric motor assists the gasoline engine at low speeds.

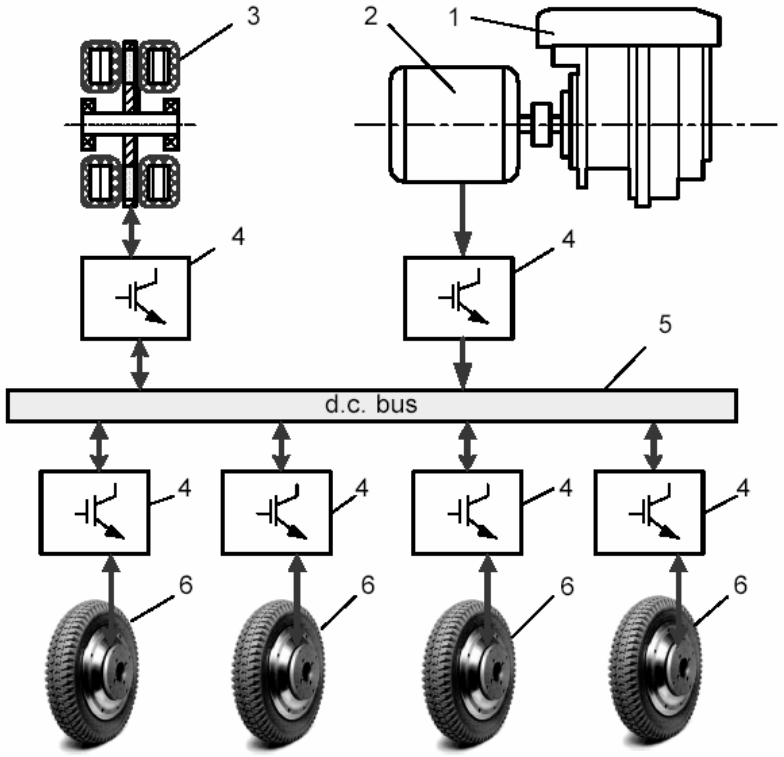

HEV with flywheel energy storage: 1 – gasoline combustion engine, 2 – brushless generator, 3 – integrated flywheel motor generator, 4 – solid state converter, 5 – d.c. bus, 6 – electrical motorized wheel.

Axial Flux Permanent Magnet Brushless Motors

Applications: Solar Powered Electric Vehicles

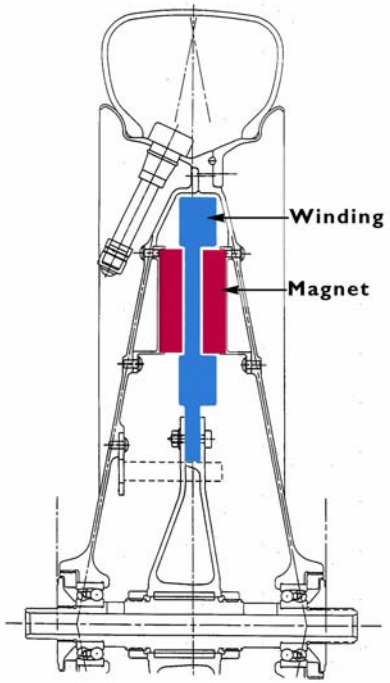

In-wheel motor

CSIRO
Australia

Stator winding

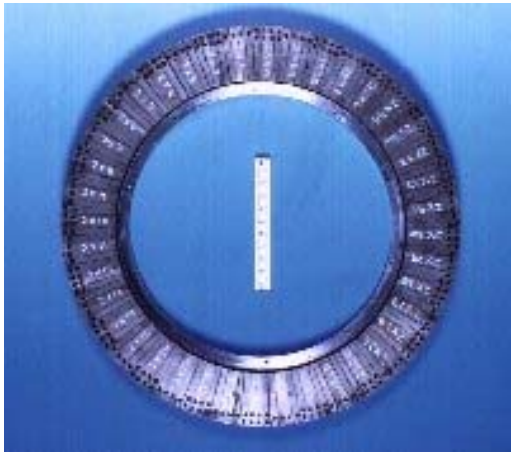

Rotor permanent magnets

***Aurora* solar powered electric vehicle with ironless PMBM (solar car race, Australia)**

Motor for *Aurora* car:	
mass of frameless motor	7.7 kg
rated torque	16.2 Nm
rated speed	1060 rpm
efficiency	98.2%

Axial Flux Permanent Magnet Brushless Motors

Applications: "Kone" MonoSpace Elevator with EcoDisk Motor

(a) sheave

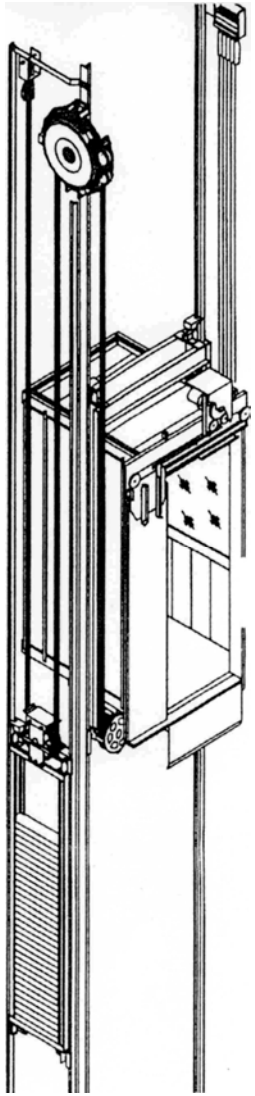

(b) *Kone* disk type
PM brushless motor

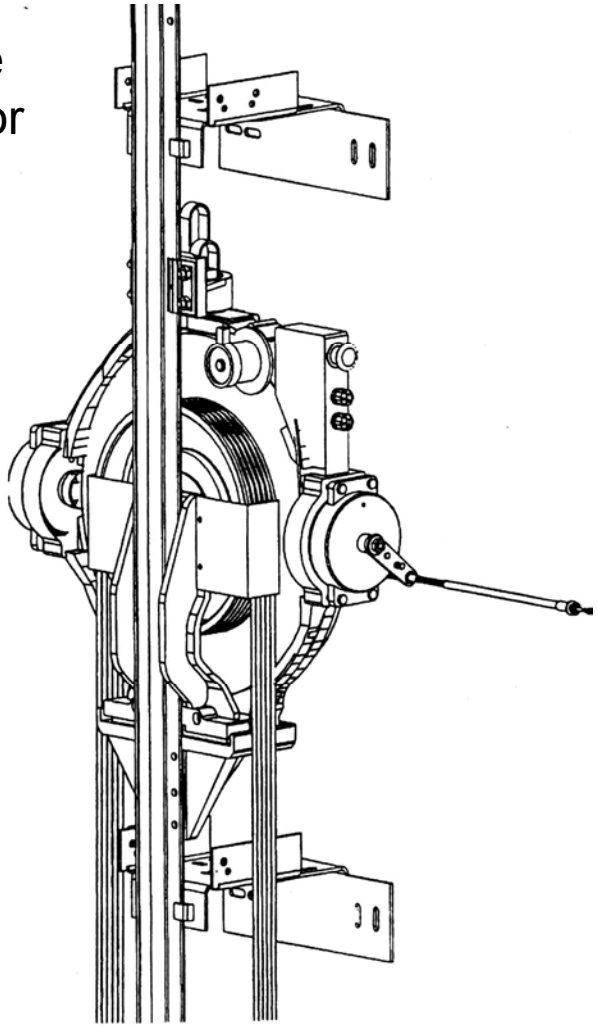

Axial Flux Permanent Magnet Brushless Motors

Applications: "Kone" MonoSpace Elevator with EcoDisk Motor

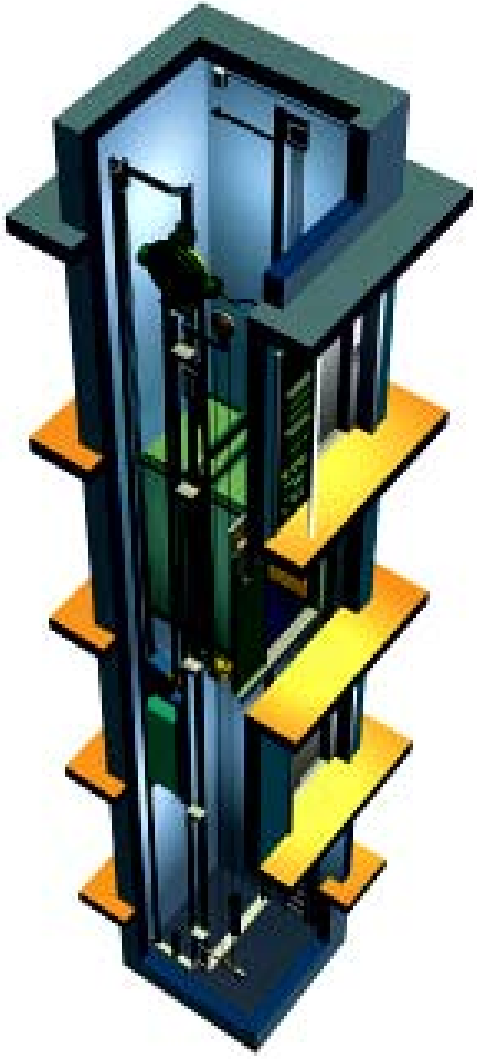

Axial Flux Permanent Magnet Brushless Motors

GM in-wheel axial flux motor

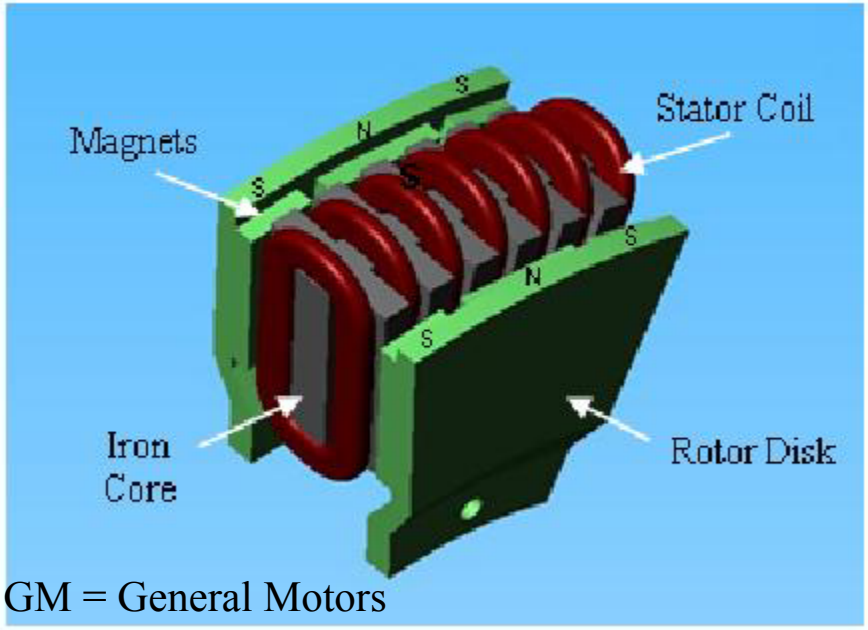

GM = General Motors

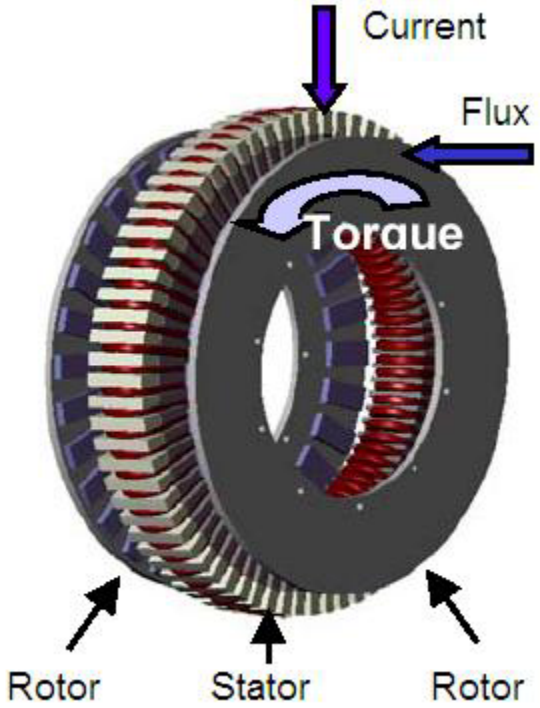

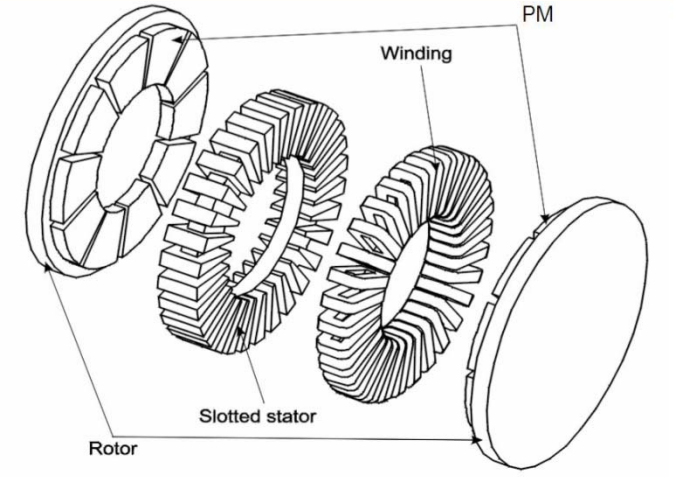

Axial Flux Permanent Magnet Brushless Motors

Conversion of bicycle

conversion kit

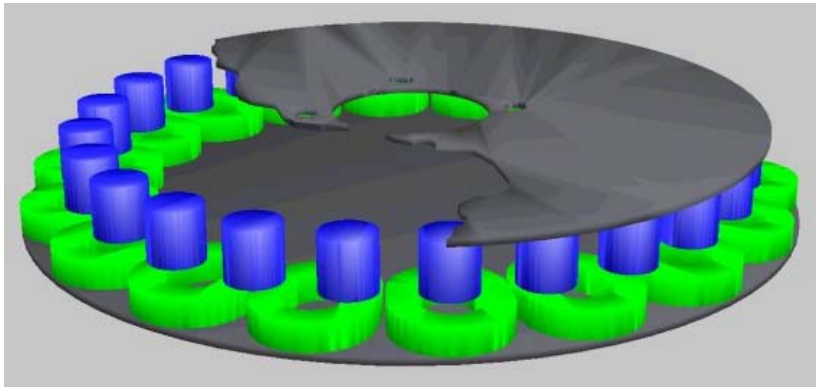

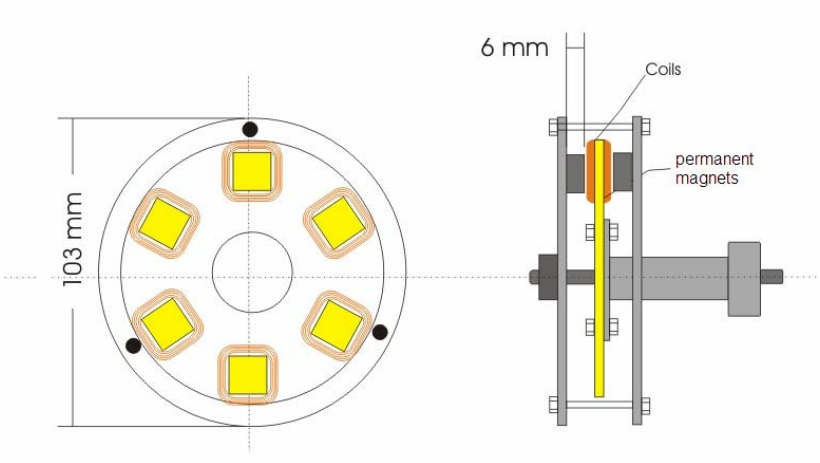

Axial Flux Permanent Magnet Brushless Motors

Homemade axial flux generator

Volvo disk brake converted into 800-W PM axial flux generator

Axial Flux Permanent Magnet Brushless Motors

Applications: Flywheel Power Module

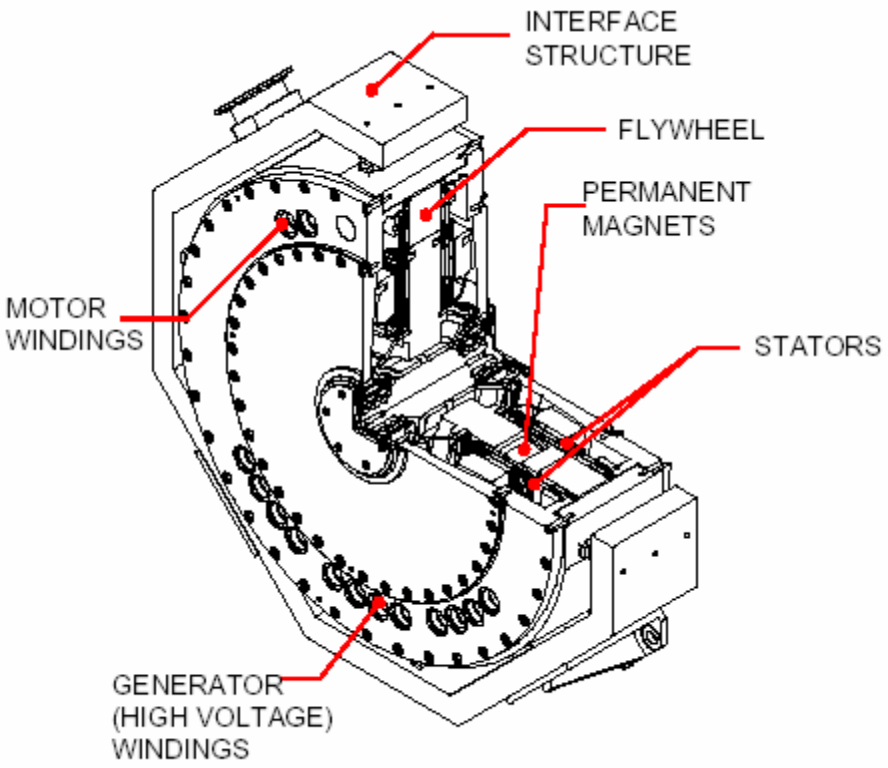

- Three Phase, Axial Gap, Permanent Magnet Machine
- Hall Switch Commutated
- Iron-less Stator
- Rotating Back-Iron
- Separate Charge (Motor) and Discharge (Generator) Coils
- Independent Specification of Charge and Discharge Voltage

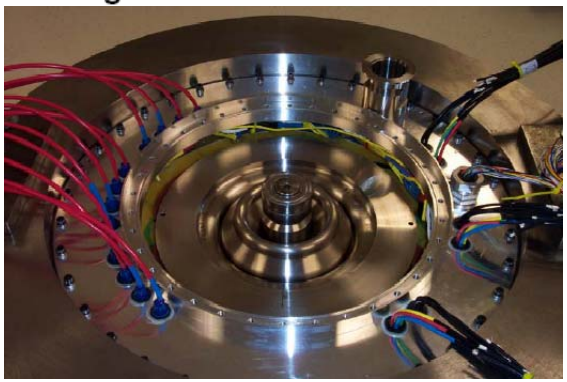

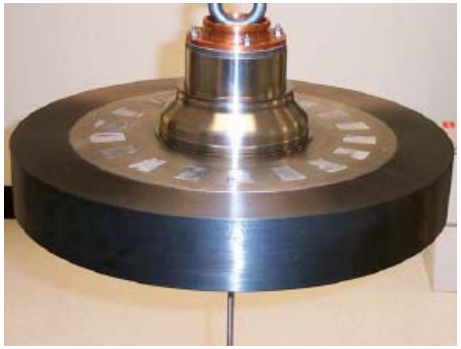

Photo Courtesy of *Optimal Energy Systems*

Axial Flux Permanent Magnet Brushless Motors

Conclusions

1. There is abundance of topologies and geometries of axial flux PM brushless motors
2. Axial flux machines have much larger diameter to length ratio than radial flux (cylindrical) machines
3. Axial flux machines can be more compact than radial flux (cylindrical) machines
4. Electromagnetic design of axial flux PM brushless motors is similar to their radial counterparts with cylindrical rotors; however the mechanical design and thermal analysis are more complex
5. Axial flux PM motors are more difficult to manufacture than cylindrical motors
6. Axial flux motors can be easy integrated with mechanical components of the drive systems, e.g. electrical vehicles, pumps, flywheels, etc.
7. Modular (multidisk) axial flux PM machine can be easily designed
8. The air gap of axial flux machines can be adjustable

Axial Flux Permanent Magnet Brushless Motors

References

1. Gieras, J.F., Wang, R.J., Kamper, M.J.: *Axial Flux Permanent Magnet Brushless Machine*. Springer-Kluwer, Dordrecht-Boston - London-, 2004.
2. Gieras, J.F.and Gieras,I.A.: *Performance analysis of a coreless permanent magnet brushless motor*. IEEE 37th IAS Meeting, Pittsburgh, PA, U.S.A., 2002.
3. Hakala, H.: *Integration of motor and hoisting machine changes the elevator business*. Int. Conf. on Electr. Machines ICEM'00, Vol. 3, 2000, Espoo, Finland, pp. 1242-1245
4. Halbach, K.: *Design of permanent magnets with oriented rare earth cobalt material*. Nuclear Instruments and Methods, Vol. 169, 1980, pp. 1-10.
5. Lovatt, H.C., Ramsden, V.S., and Mecrow, B.C.:*Design of an in-wheel motor for solar-powered electric vehicle*. Proc. IEE, EPA, vol. 145, No. 5, pp. 402-408.

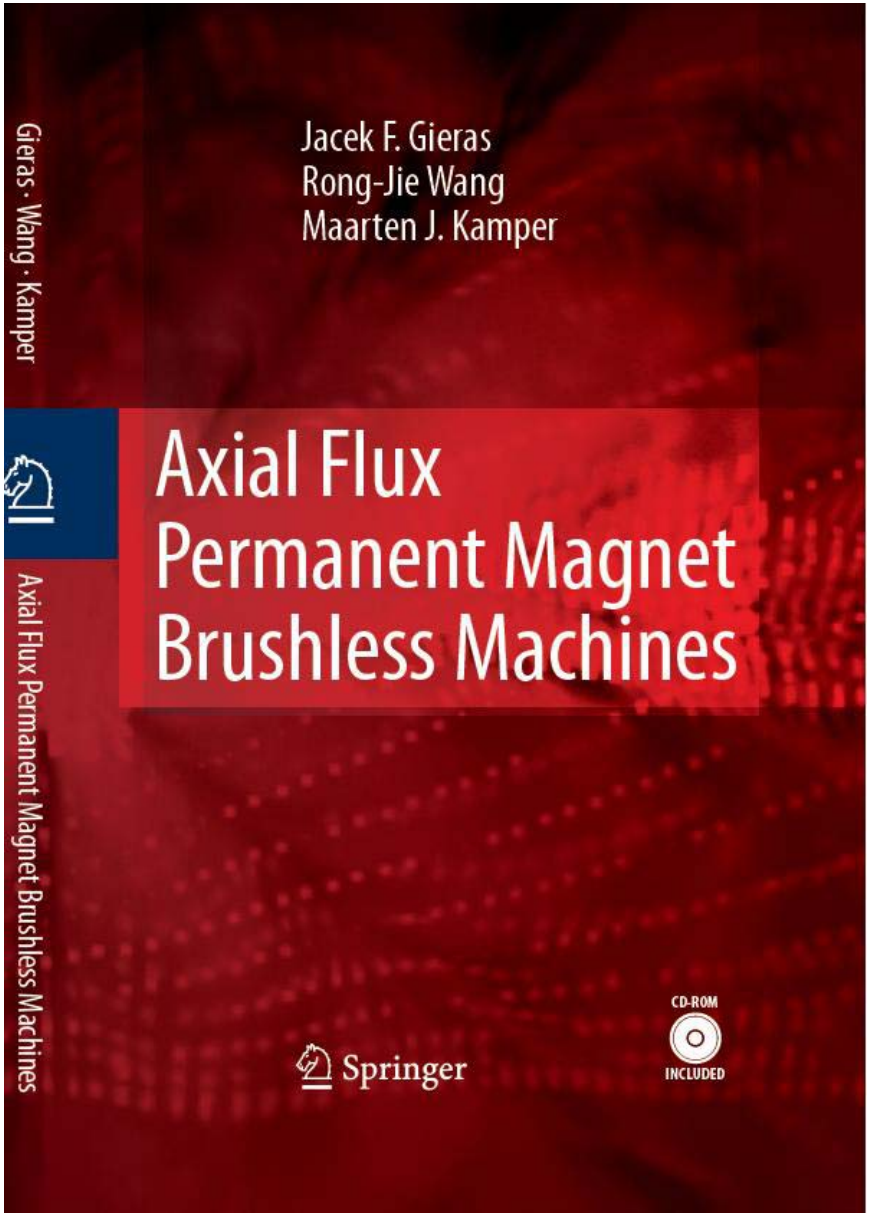

Questions

&

Answers